

Shengqian Zhou<sup>1</sup>, Ying Chen<sup>1</sup>, Shan Huang<sup>2,3</sup>, Guipeng Yang<sup>4</sup>, Honghai Zhang<sup>4</sup>, Adina Paytan<sup>5</sup>, Hartmut Herrmann<sup>3</sup>, Alfred Wiedensohler<sup>3</sup>, Laurent Poulain<sup>3</sup>, Haowen Li<sup>1</sup>, Fanghui Wang<sup>1</sup>, Yucheng Zhu<sup>1</sup>, Tianjiao Yang<sup>1</sup>

<sup>1</sup>Department of Environmental Science and Engineering, Fudan University, Shanghai 200433, China. <sup>2</sup>Institute for Environmental and Climate Research, Jinan University, Guangzhou, Guangdong 511443, China. <sup>3</sup>Leibniz Institute for Tropospheric Research, Leipzig, Sachsen 04318, Germany. <sup>4</sup>College of Chemistry and Chemical Engineering, Ocean University of China, Qingdao, Shandong 266100, China. <sup>5</sup>Institute of Marine Sciences, University of California Santa Cruz, Santa Cruz, CA 94064, USA

## Introduction

- Marine biogenic sources contribute substantially to the atmospheric gaseous and particulate components and exert significant environmental and climatic effects. Oceanic organism-derived dimethyl sulfide (DMS) is the largest natural contributor to the global atmospheric sulfur budget.
- MSA is an important product of DMS in the atmosphere, which is usually used as a tracer for marine biogenic aerosols. However, whether it is valid has not been carefully verified.
- Establishing the linkage between MSA and sea surface phytoplankton is of great significance for studying the ocean-atmosphere interactions and understanding the role of marine phytoplankton in aerosol-cloud-climate feedback system.
- Revealing the spatial and temporal distributions of MSA is vital for understanding related environmental effects.

## Materials and Methods

### Aerosol MSA observation

- the Atlantic Ocean, 2011 – 2012
- Huaniao Island (HNI), 2013 – 2018
- the Gulf of Aqaba (GA), 2003 – 2005
- west North Pacific Rim (NWPR), 2009 – 2018

### AEC calculation

$$AEC = \frac{\sum_{i=0}^{72} Chla_i \cdot e^{-\frac{t_i}{72}} \cdot \frac{600}{BLH}}{n}$$

$n$ : the tracking time of endpoint  $i$   
 Mean MODIS Chl- $a$  concentration around the trajectory endpoint  $i$

### Others

HYSPLIT trajectory, Empirical Orthogonal Function (EOF) analysis

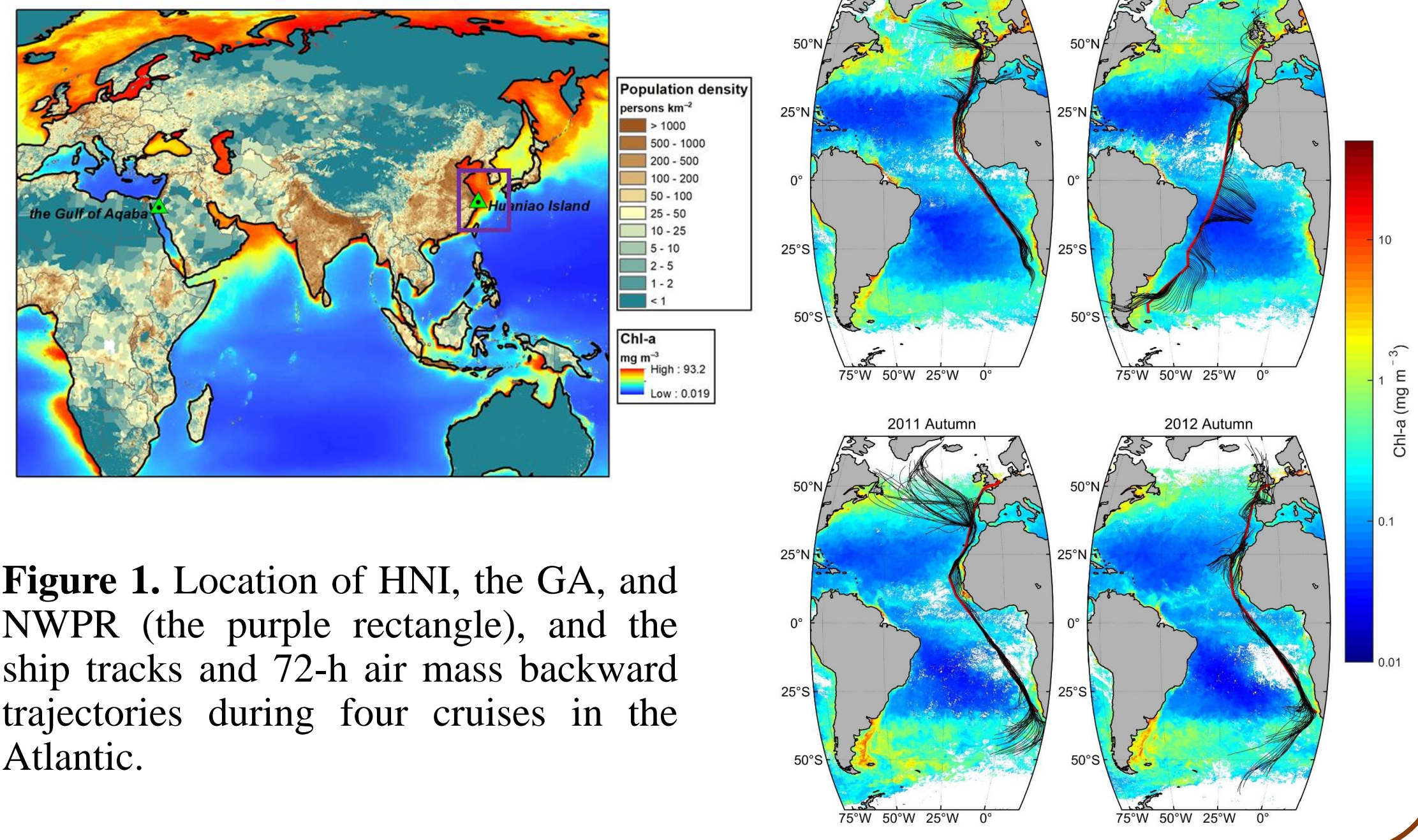


Figure 1. Location of HNI, the GA, and NWPR (the purple rectangle), and the ship tracks and 72-h air mass backward trajectories during four cruises in the Atlantic.

## AEC can be correlated with MSA in mid-latitude Northern Hemisphere

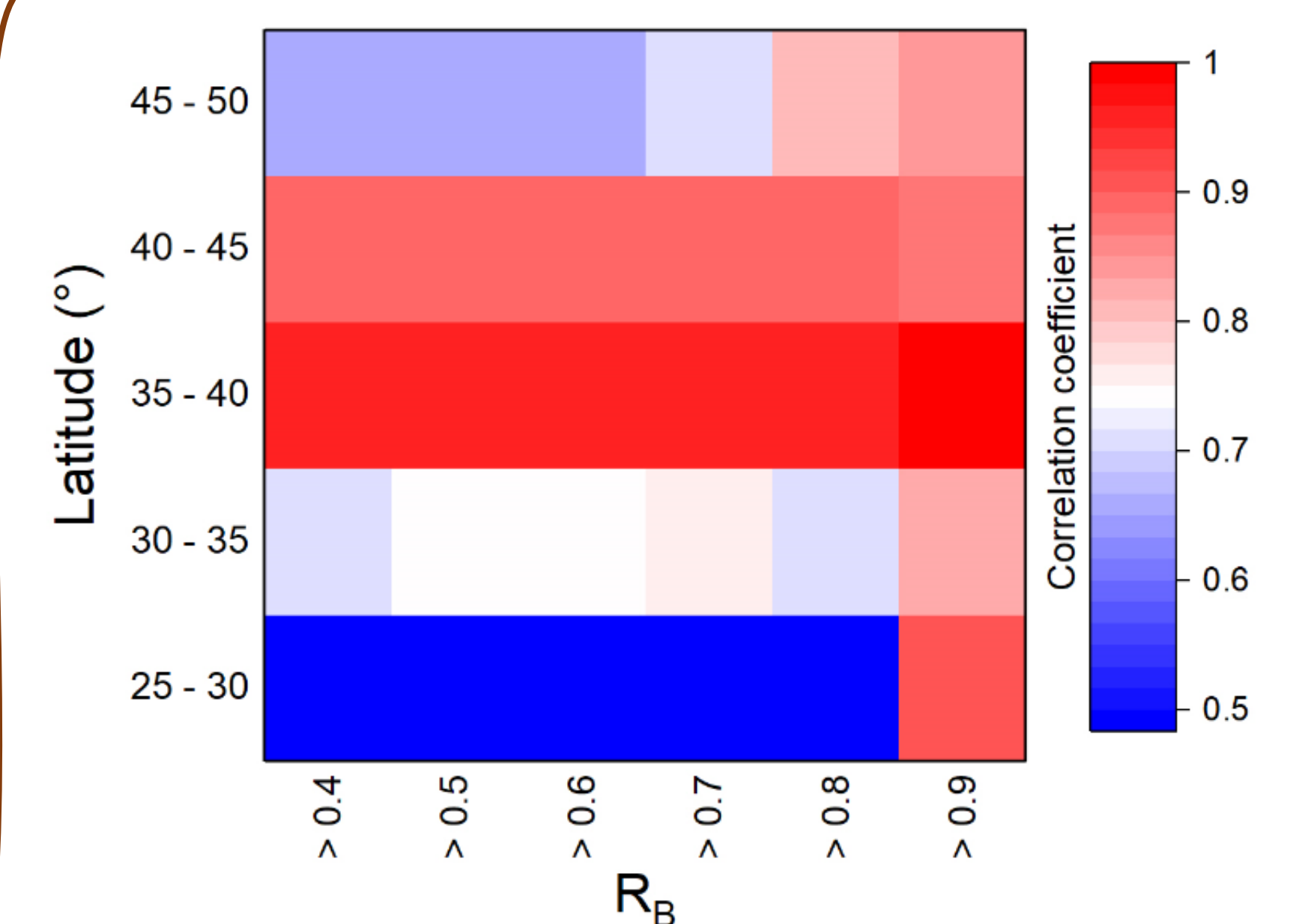


Figure 4. Correlation coefficient matrix of MSA concentration and AEC in different latitudes and different  $R_B$  ranges.

## Influence of transport pattern and perturbation of terrestrial sources

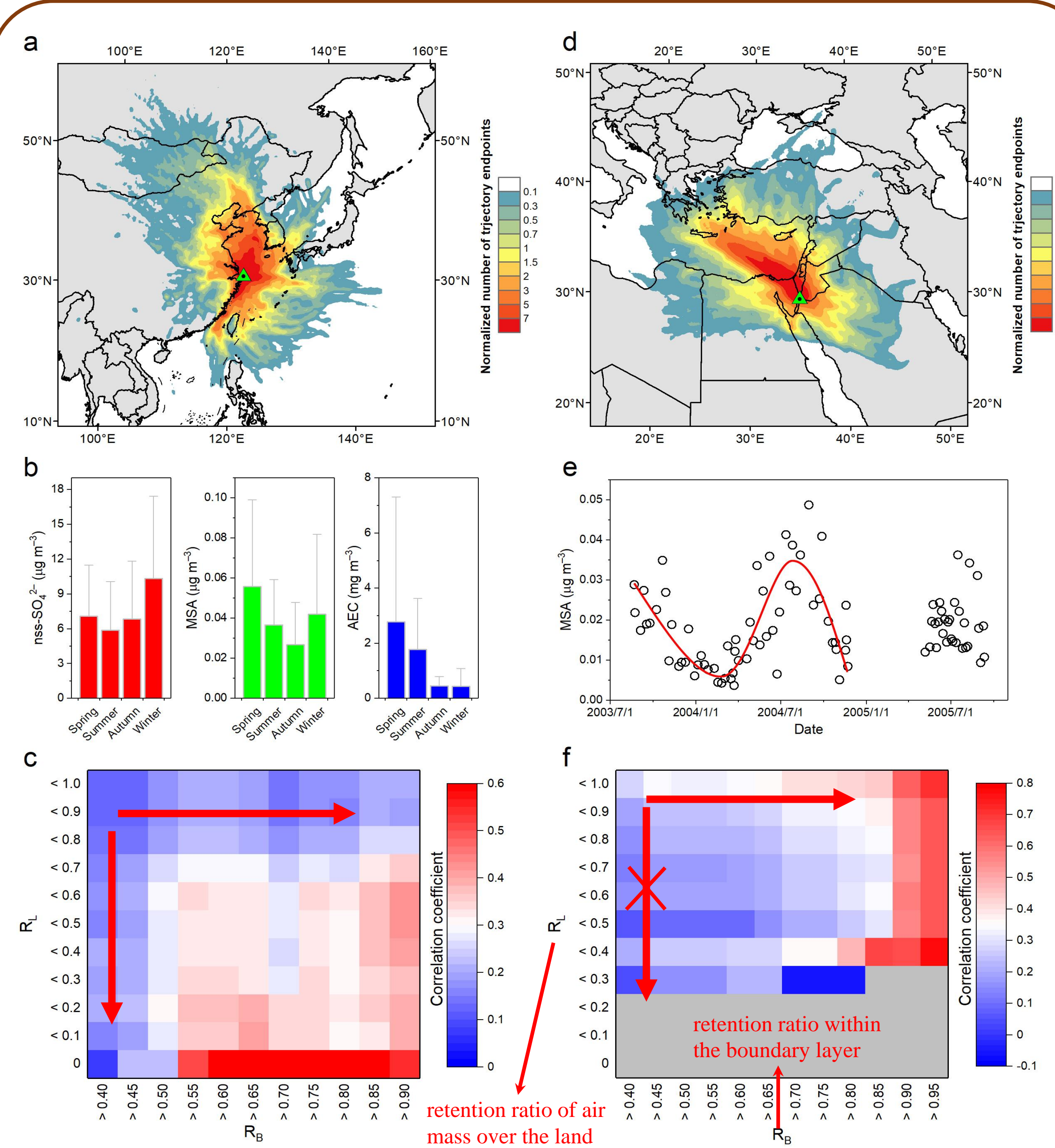


Figure 2. **a** and **d**, The spatial distribution of main source regions for HNI (**a**) and the GA (**d**). **b**, Seasonal variations of  $nss-SO_4^{2-}$ , MSA and AEC for HNI. **c** and **f**, Correlation coefficient matrix of MSA concentration and AEC in different  $R_L$  and  $R_B$  ranges for HNI (**c**) and the GA (**f**). **e**, Time series of MSA concentration for the GA.

- HNI**: The correlation between MSA concentration and AEC is significantly enhanced with the filtration of  $R_L$  to low level.  $\rightarrow\rightarrow$  the nonnegligible contribution of terrestrial sources to MSA  $\rightarrow\rightarrow$  the abnormally high MSA concentration in winter
- the GA**: No influence of  $R_L$  on correlation between MSA and AEC and the typical seasonal cycle of MSA concentration (summer > winter)  $\rightarrow\rightarrow$  no contribution of terrestrial source
- Both two sites**: The correlations between MSA and AEC increase with the filtration of  $R_B$  to high value.  $\rightarrow\rightarrow$  Atmospheric components can be linked to sea surface of source region only when the movement of air masses is mostly confined within the marine boundary layer.

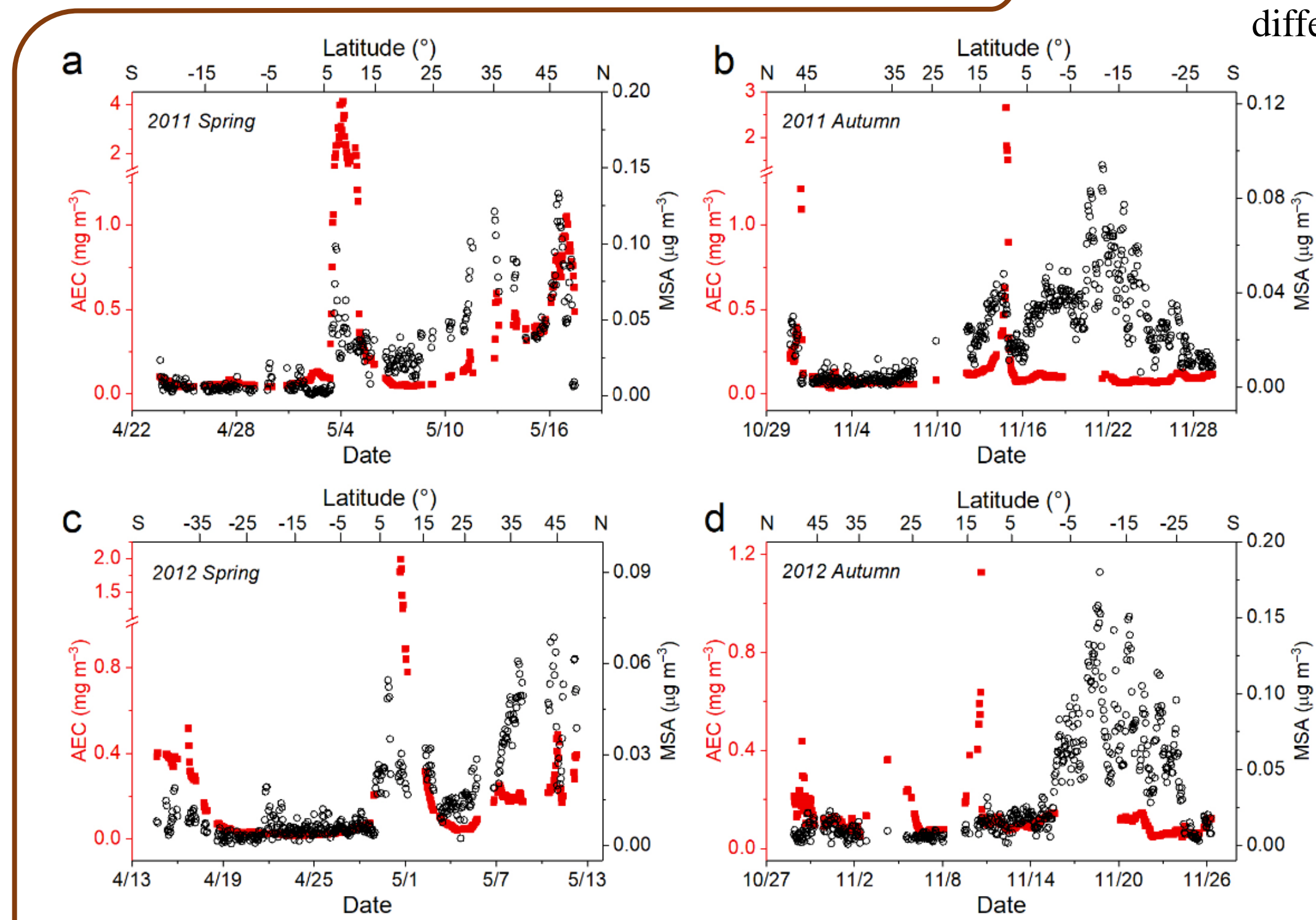


Figure 3. Time series of MSA concentration and corresponding AEC over the Atlantic during four cruises in 2011 and 2012.

- MSA correlated with AEC in the North Atlantic, but not in the South Atlantic
- predominance of DMS-related algae species (coccolithophores)
- Closer linkage between MSA and surface phytoplankton under high  $R_B$  is a universal principle

## Simulation of the distribution of ocean-derived MSA

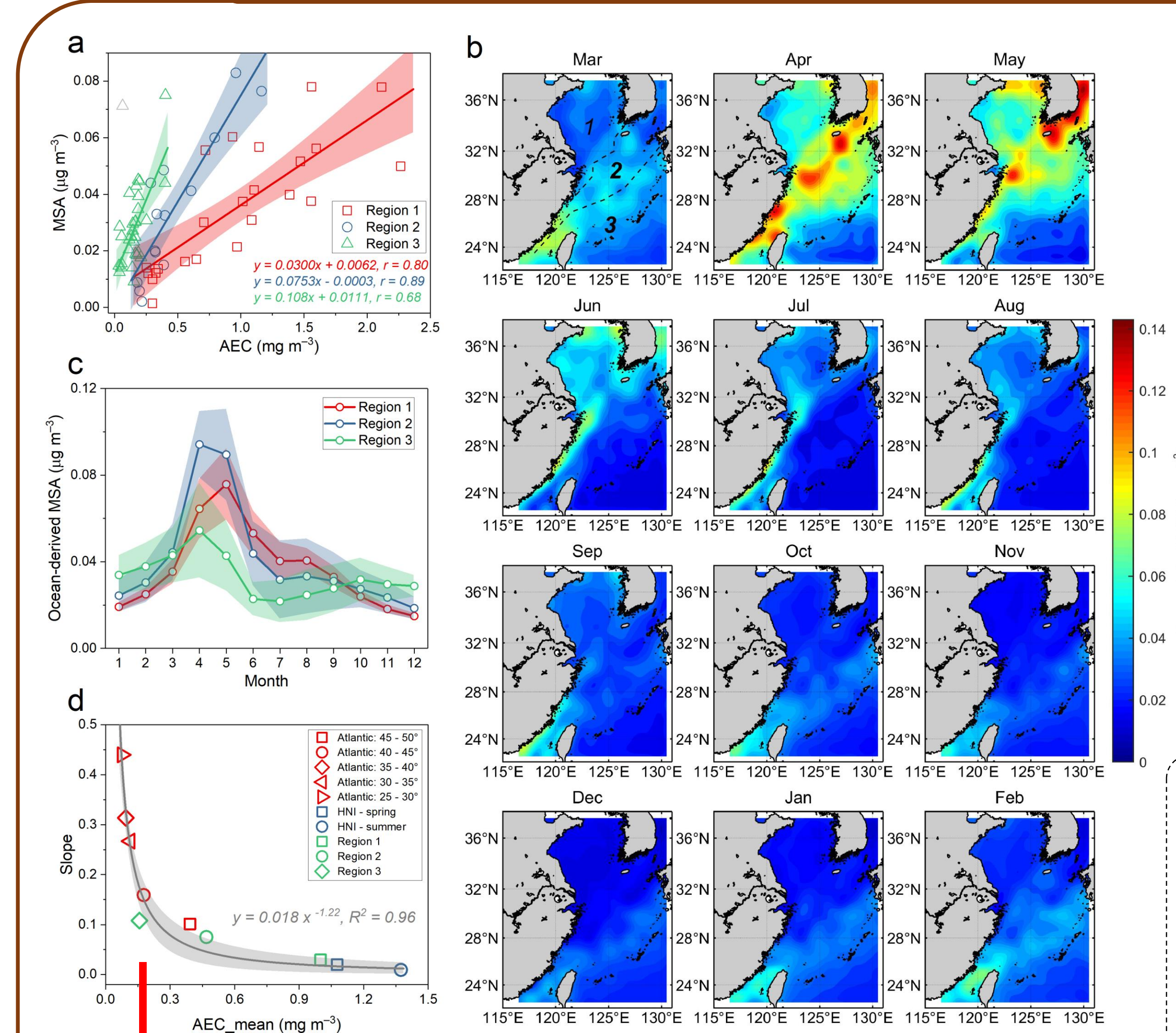


Figure 5. Simulation of ocean-derived MSA over the WNPR. **a**, Correlations between measured MSA concentration and AEC index in each region. **b**, Monthly climatology of simulated ocean-derived MSA over the WNPR. **c**, The average concentrations of simulated ocean-derived MSA for each region in different months. **d**, The relationship between the linear fitting slopes of MSA concentration versus AEC and the mean values of AEC ( $AEC_{mean}$ ) for different regions.

### A negative relationship

- This good nonlinear curve fitting result can be applied to MSA simulation in large scale
- The quantitative relationship between phytoplankton and atmospheric biogenic sulfur it produces will change with the change of overall phytoplankton biomass.

- NWPR was divided into 3 regions based on 10-year AEC grid dataset by *K-means* approach.
- For each region, there is a good correlation between AEC and MSA.  $\rightarrow\rightarrow$  be used to simulate the spatiotemporal distribution of ocean-derived MSA

E-mail [yingchen@fudan.edu.cn](mailto:yingchen@fudan.edu.cn)